On measuring interface loads in structural full scale testing - planning, calibration, and data processing

CASI AERO 2021 – 26th CASI Aerospace Structures & Materials Symposium

Calista Biondic [1,3]
calista.biondic@nrc-cnrc.gc.ca *OR* calista.biondic@mail.utoronto.ca
Stéphane Brunet [2] **Yan Bombardier** [2] **Catherine Cheung** [2]
Stephane.brunet@nrc-cnrc.gc.ca yan.bombardier@nrc-cnrc.gc.ca catherine.cheung@nrc-cnrc.gc.ca
[1] *Full-time undergraduate at University of Toronto – National Research Council of Canada Co-op Student*
[2] *National Research Council of Canada*
[3] *Corresponding author*

***Abstract* – Full scale testing has continually played an integral role in aircraft structural analysis, safety, and certification. In combination with instrumentation techniques like strain gauges, digital image correlation (DIC), fibre optic strain measurements, and others, full-scale testing is an important tool to better understand the aircraft structure behaviour under representative flight loads. Government agencies have relied on full scale testing results to support the approval of life extensions, physical modifications, or usage changes.**

In collaboration with the Royal Canadian Air Force, the National Research Council of Canada (NRC) has completed a durability and damage tolerance test of the CF-188 inboard leading edge flap (ILEF), as part of a life extension program for the CF-188 flight control surfaces.

For this test, a reaction structure was built to hold a right-hand-side wing on which the ILEF test article was mounted. A set of lugs simulating the fuselage bulkheads were designed to interface directly with the inner wing root lugs. These custom lugs were instrumented with strain gauges, with the intent of estimating the load distribution at this interface with the reaction structure. Prior to their final installation on the reaction structure, they were individually calibrated in a load frame with vertical and horizontal loads applied. This paper focuses on the techniques used to select the gauge locations and orientations, the calibration procedure, and the data analysis. Finally, some lessons learned from this project are discussed.

Keywords: CF188, F/A-18, ILEF, full scale test, instrumentation

1. Introduction

Full scale testing has continually played an integral role in aircraft structural analysis, safety and certification. In combination with instrumentation techniques like strain gauges, digital image correlation (DIC), fibre optic strain measurements, and others, full-scale testing is an important tool to better understand the aircraft structure behaviour under loads experienced in flight. Government agencies have relied on full scale testing results to support the approval of life extensions, physical modifications or usage changes.

As part of the Canadian F/A-18 Hornet (CF188) control surfaces life extension program, a durability and damage tolerance fatigue test (DADTT) followed by a Residual Strength Test (RST) were carried out on the inboard leading edge flap (ILEF) by NRC, using service representative loads.

For this test, illustrated in Figure 1, a reaction structure was built to hold a right-hand-side wing on which the ILEF test article was mounted. A set of lugs simulating the fuselage bulkheads were designed to interface directly with the inner wing root lugs at fuselage stations (FS) 453, 470.5, and 488, as shown in Figure 2. The wing assembly was also connected to the reaction structure through a vertical shear-only reaction point at FS 508 and the drag load member. The custom lugs were instrumented with strain gauges, with the intent of estimating the load distribution at this interface with the reaction structure.

The load frame wing root lugs were designed to meet the strength and fatigue performance requirements in order to complete the ILEF fatigue test without load frame failure. Based on these requirements, the resulting lug designs were very stiff, which is typically an advantage for load frame parts. However, it was anticipated that the strain gauges may not be sufficiently sensitive to determine the lug loads with an acceptable level of accuracy, as the measured strains should be significantly larger than the typical noise recorded. To improve the probability of reliable strain measurements, three-dimensional finite element analyses (FEA) of the stiffer lugs was used to determine the optimum location of the strain gauges.

The load distribution among the custom lugs can only be estimated by analysis or by deriving the loads from strain gauge measurements. To achieve the latter, the response of the gauges must be properly calibrated under known loads prior to test start. Two calibration setups were designed to load each pair of lugs along the vertical and horizontal directions. Using the strain gauge measurements and loads recorded during calibration, regressions for the horizontal and vertical load experienced at each lug were created.

The regression models built were then used to estimate loads experienced during the testing, focusing on two specific load conditions inducing maximum and minimum wing root bending moment (WRBM) respectively. As a way to verify the accuracy of the models, the loads from the regressions were used to calculate bending moment and torsion, and compared to the values produced by the actuators. A second goal was to verify if the drag load member may be experiencing loading in unexpected directions.

This paper discusses each of the analysis steps in detail, focusing on the following tasks: specification of strain gauge requirements (quantity and location) using finite-element analysis, calibration of root lug fittings, development of load transfer functions, and quantification of the accuracy of these functions.

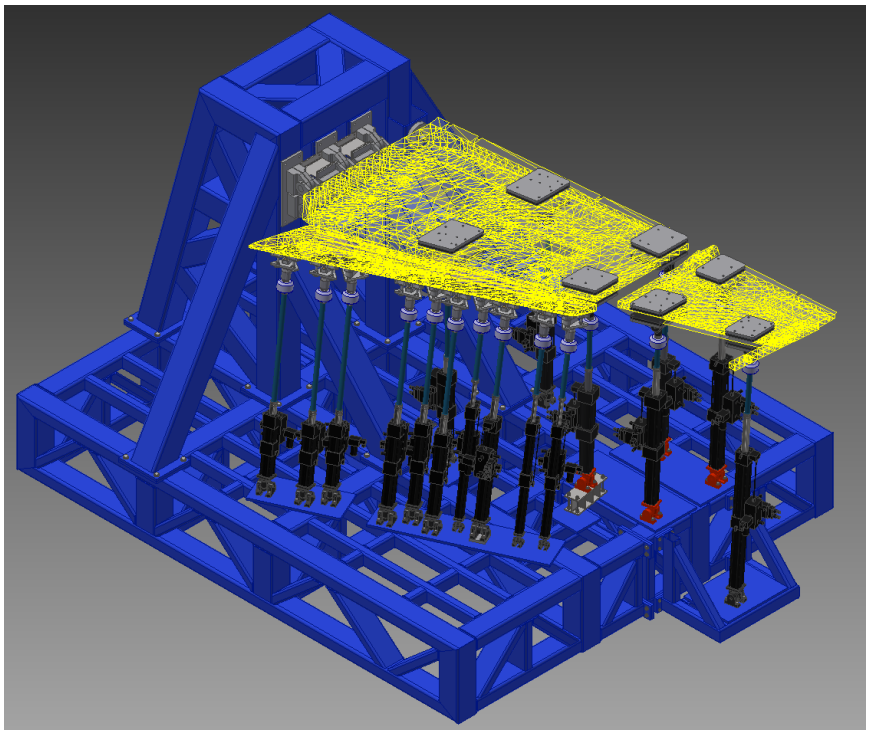

Figure 1: CF-188 ILEF Test Rig with the Wing Mounted Upside Down

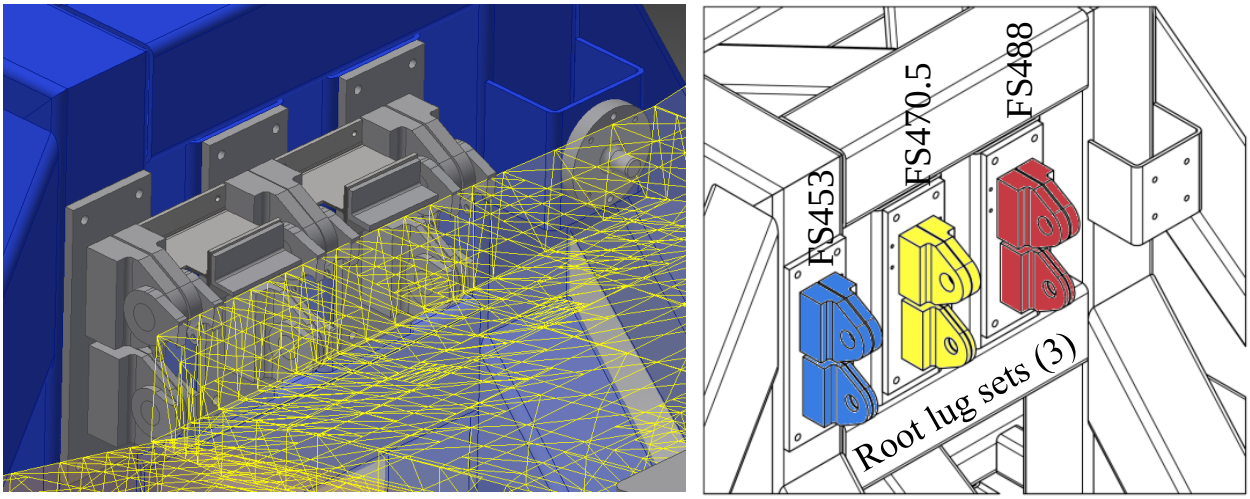

Figure 2: Details of the Wing Root Interface

2. Determination of Strain Gauge Locations

The first step in this methodology was to determine appropriate locations for strain gauges on the custom lugs. Due to hardware limitations of the data acquisition system, the total number of strain gauge channels could not exceed four quarter-bridge channels for each of the six pairs of lugs shown in Figure 2.

The location of the strain gauges was determined by conducting three-dimensional (3D) finite element analyses (FEA) of the stiffer load frame lug, which was the one where strain measurements were expected to be the lowest.

A 3D solid model was built in the FEA program StressCheck version 10.3 which uses *p*-element formulation. Frictionless contact analysis was modelled between the pin and the lug. Hoop and radial strains around the lug were then extracted for three load cases: tensile load (PULL00), compressive load (PUSH00), and transverse load (PULL90). The three load cases are illustrated in Figure 3. Finally, the number, location, and orientation of the strain gauges were selected by maximizing the magnitude of the strain measurements for the three tested load cases.

Note that the strain values documented in this section were calculated by applying 10,000 lbf per lug, which is equivalent to a load of 20,000 lbf per pair of lugs.

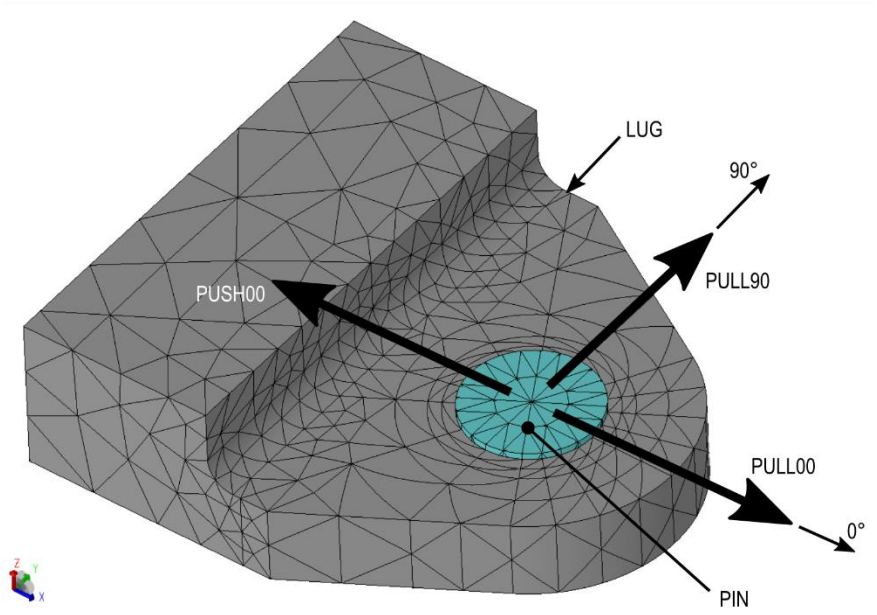

Figure 3: Tetrahedral Mesh and Load Cases

FINITE ELEMENT ANALYSIS RESULTS

The radial and hoop strain results are presented in Figure 4. The analysis of the results shows that:

- The maximum compressive radial strains are located at the contact region between the pin and the lug. Note that the maximum compressive radial strain for the PULL90 load case is located at approximately 135° while the pin load was applied at 90°. This is due to the fact that the contact region is shifted towards the stiffer region of the lug (thicker section with lug attachment points).
- Determining the pin load by monitoring radial strains may not be optimal as the compressive radial strains caused by the contact between the pin and the hole is typically localized. Also, the gap between the pin and the hole may have a significant impact on the size and magnitude of the localized compressive zone. However, the hoop strains around the hole are low for the PUSH00 load case (less than 100 microstrains for the applied load). Consequently, monitoring the radial strains at 180° might be the best approach to determine the compressive loads from the PUSH00 load case.
- For the PULL00 and PULL90 load cases, the magnitude of the measured strains tend to be higher along the hoop direction.

RECOMMENDED STRAIN GAUGE LOCATIONS

Hoop and radial polar strain plots, illustrated in Figure 5, were very useful at quantifying and identifying the optimal strain gauge orientations and locations around the hole. These plots were used to assess the effects of angular position and radial distance on the measured strains. One of the main takeaways was that the strain decreases with edge distance. This led to the selection of a strain gauge radial position located at 0.470 inch from the edge of the hole. This presented the best compromise between sensitivity and the risk of the shims rubbing and damaging the gauges.

The magnitude of the measured strains vary as a function of angular position and load direction. Based on the information presented in Figure 5, the recommended strain gauge locations and orientations were determined for each of the three load cases.

The final strain gauge locations is illustrated in Figure 6 were selected for the following reasons:

- Strain Gauge 4: Measures hoop strains caused by the PULL00 load case.
- Strain Gauges 1 and 3: Measures hoop strains caused by the PULL90 load case and its reverse direction. While the optimal angle was around 130° for the PULL90 load case, it was decided to locate them at 120° to measure higher strains under the PULL00 load case. Consequently, strain gauges 3 and 1 are located at 120° and 240° respectively.
- Strain Gauge 2: Measures radial strains caused by the PUSH00 load case.

Variation of the Measured Strains as a Function of Loading Direction

The loads expected during the test are dominated by the PUSH00 and PULL90 load cases (aligned along the 0°-180° axis). The shear component (along the 90°-270° axis), represented by the PULL90 load case, is expected to be lower. It was planned to perform a linear regression of the data to calculate the load components (magnitude and direction) from strain gauge measurements. However, it was also anticipated that the strain responses would be non-linear due to the contact and the geometry of the lug.

Figure 7 shows the simulated strain gauge measurements calculated using the finite element model by varying the load direction from 0° to 180° by 10° increments. With the exception of Strain Gauge 2, all gauges show an approximatively sinusoidal behaviour.

Strain Gauge Naming Convention

The following naming convention was adopted for the strain gauges: three letters designating an upper root lug gauge (URG) or a lower root lug gauge (LRG), followed by three digits designating the lug fuselage station (453, 470 or 488), and ending with the strain gauge number (1,2,3, or 4 as defined in Figure 6).

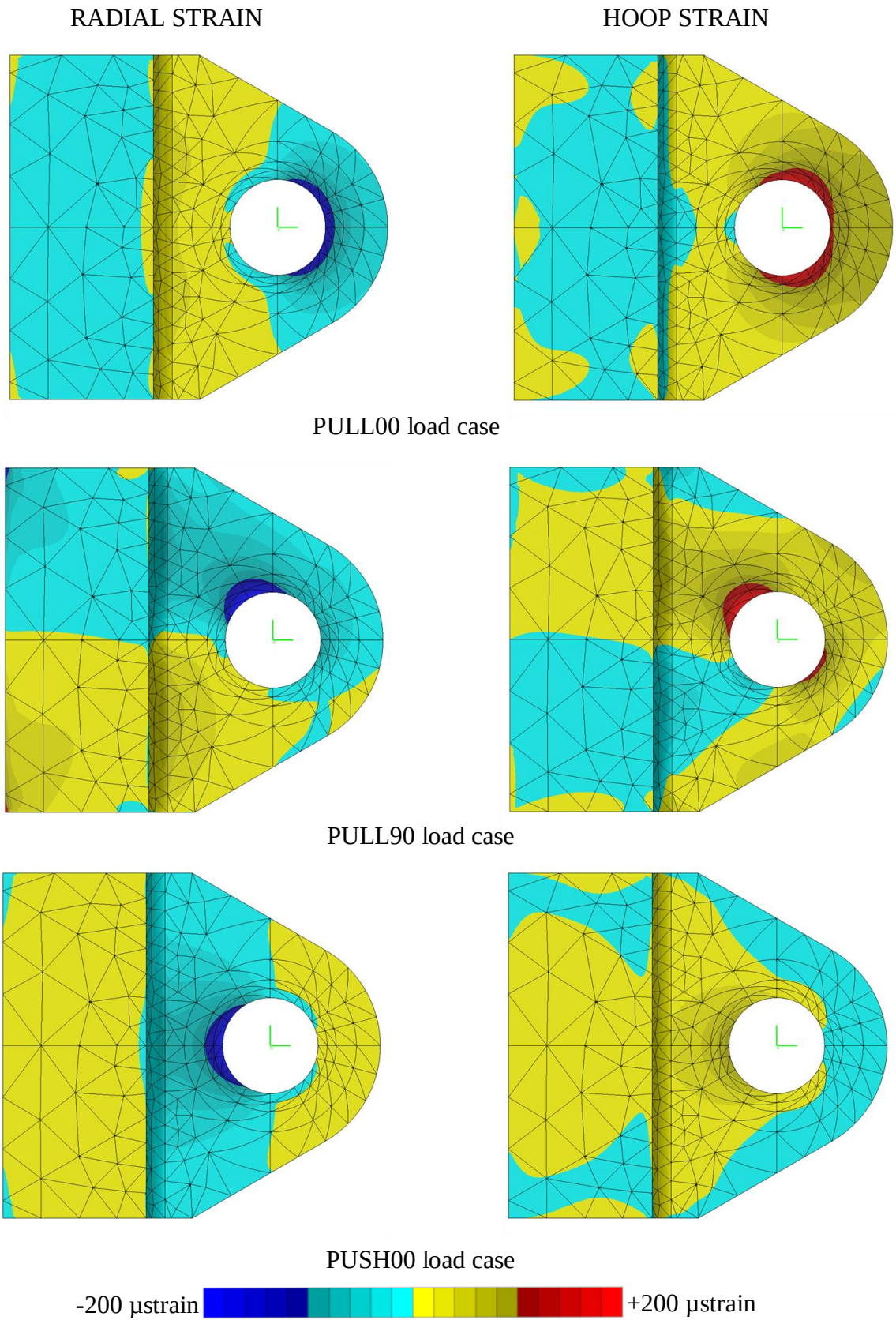

Figure 4: Radial and Hoop Strain Results

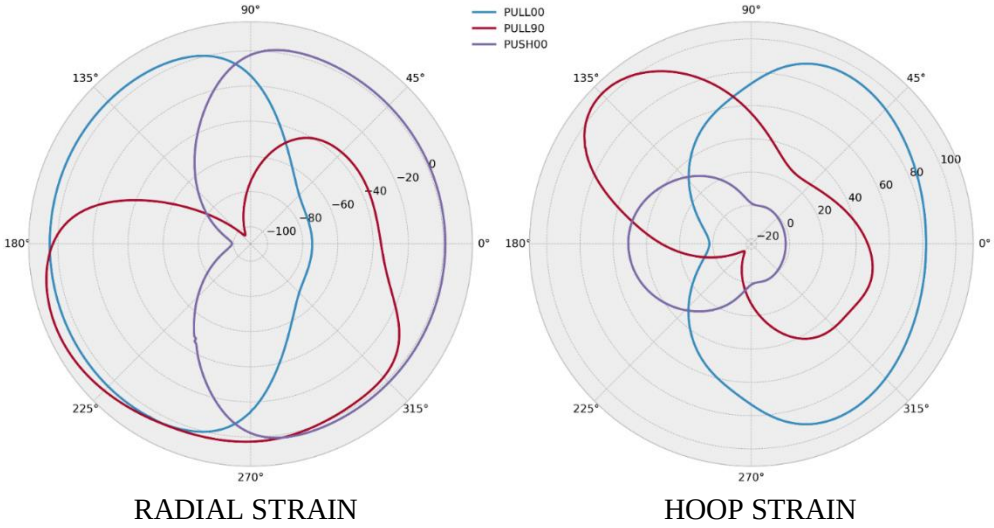

Figure 5: Radial and Hoop Strains for All Load Cases Along a Ring Located at 0.470 inch from the Edge

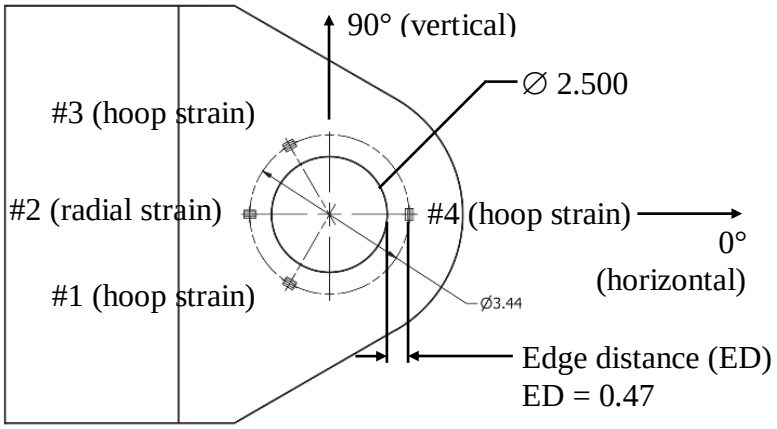

Figure 6: Final Strain Gauge Locations (Dimensions in inches)

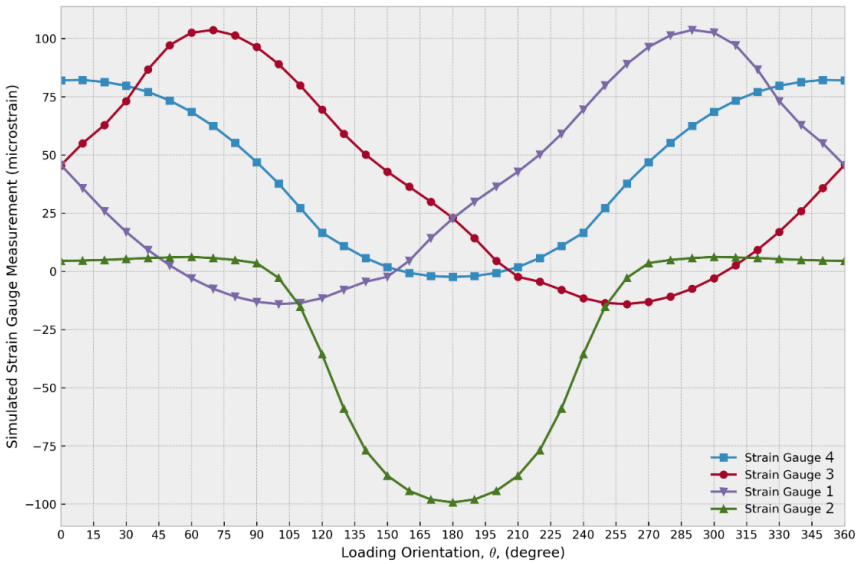

Figure 7: Simulated Strain Gauge Measurements as a Function of Loading Direction

3. Calibration

The calibration step in this methodology was required to capture the strain gauge response to known load values in both horizontal and vertical directions. For this purpose, two calibration setups were designed to load each pair of lugs along the vertical and horizontal directions, as illustrated in Figure 8.

Ideally, calibration loads would have been chosen to cover the full range of loads carried through the lugs during the test (±310 kip and -65/+25 kip in the horizontal and vertical direction respectively), but due to practical considerations, the best achievable calibration range was ±35 kip for both directions.

For each lug pair, a loading sequence was applied in tension and compression, for both directions, which consisted of a ramp from zero load to the maximum load magnitude, in steps of 10% of the maximum calibration load. At each step, the ramping was paused for approximately 60 seconds prior to recording of the strain gauge readings. After the maximum magnitude load was reached, the load was brought back directly to zero without further recording of strain gauge data.

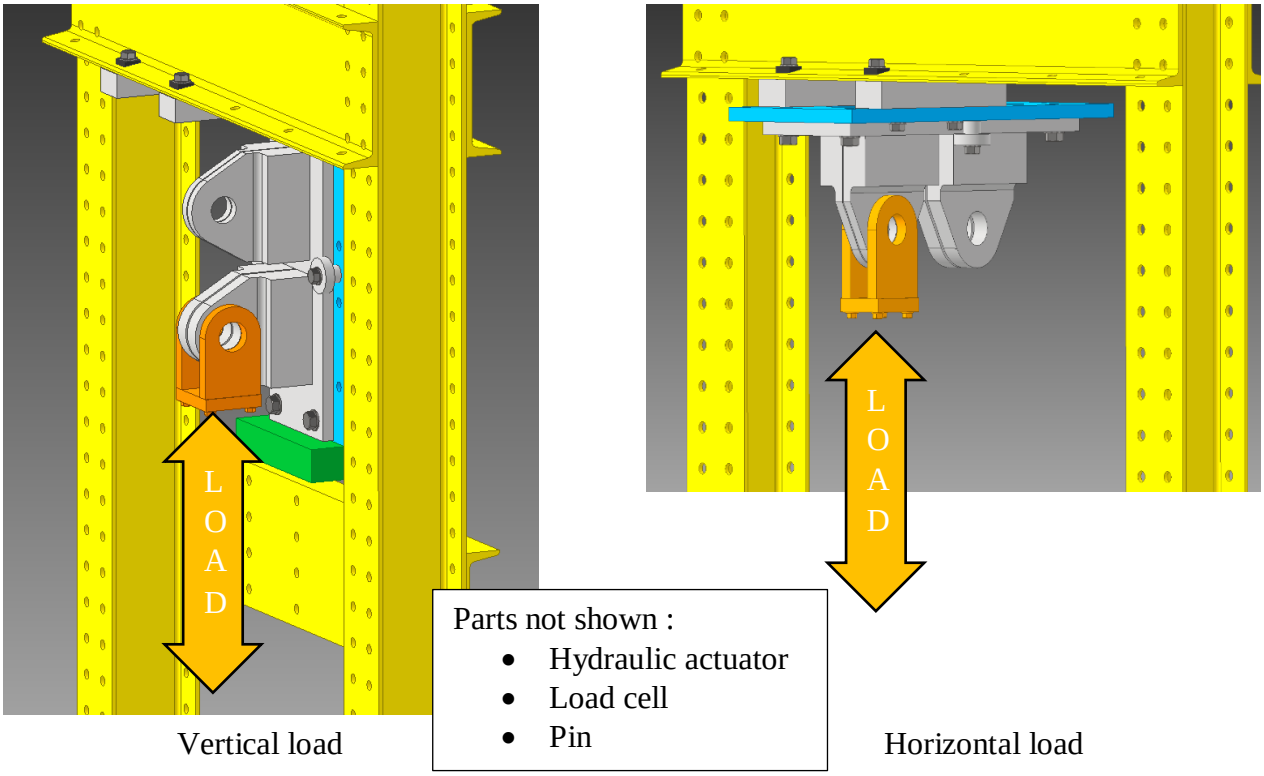

Figure 8: Calibration Setup

4. Data Analysis

During the calibration process discussed in the previous section, strain gauge measurements and applied loads were recorded for each set of lugs at the three fuselage stations. This data was then used to create linear regression models that relate the strain readings to the horizontal and vertical loads experienced at each location. Based on information gathered from the load vs. strain plots, several approaches with varying number of strain gauges were used to create the linear regressions.

Load vs. Strain Plots

The plots showing calibration load vs. strain were produced to visualize the response of the four strain gauges of each lug. Since the goal is to create linear regression models, it is interesting to note that many of the plots show non-linear responses to the calibration loads. A majority of the strain gauges show close to bi-linear behaviour for horizontal loads, with different slopes for negative and positive loads. Non-linear strain responses were more visible for the vertical load case. Figure 9 shows an example of nearly-perfect bi-linear behaviour on the upper lug at FS453 whereas Figure 10 shows an example of undesirable highly non-linear behaviour on the upper lug at FS470.

Another interesting trend identified was that Strain Gauge 2 on all six of the lugs showed to be most responsive to negative horizontal loads, while its strain readings for positive horizontal loads and all vertical loads were much less significant.

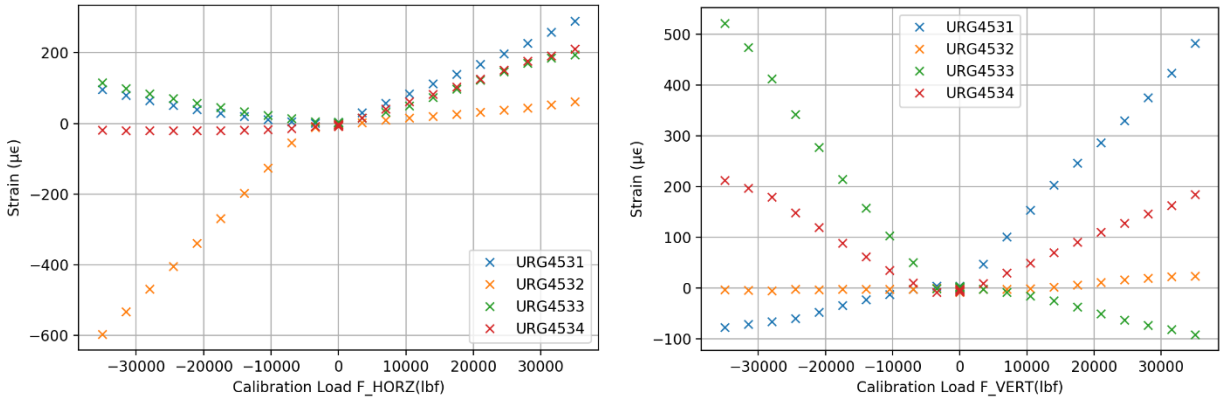

Figure 9: Horizontal (Left) and Vertical (Right) Load vs. Strain for the Upper Lug at FS453

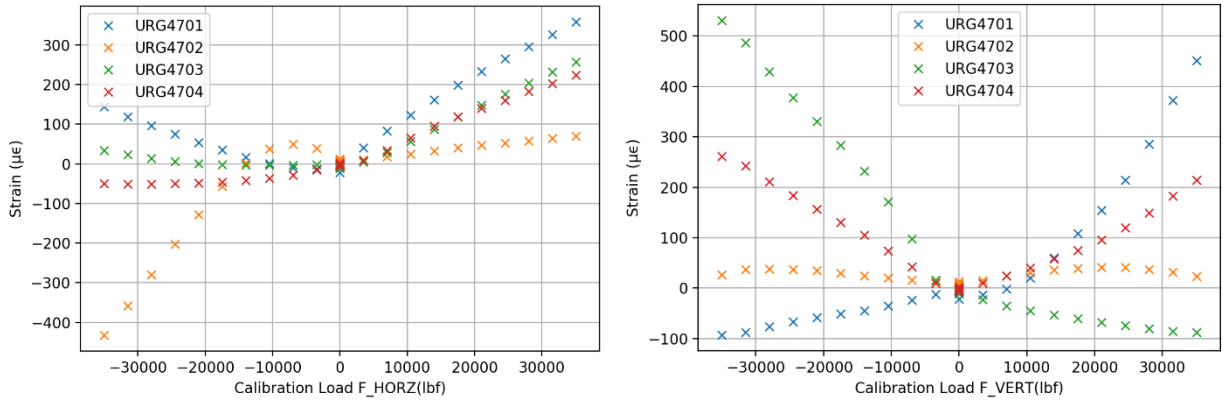

Figure 10: Horizontal (Left) and Vertical (Right) Load vs. Strain for the Upper Lug at FS470

SINGLE-EQUATION FOUR-GAUGE REGRESSIONS

The first approach was to utilize all four available strain gauges to build models for the horizontal and vertical loads for the upper and lower lug at each fuselage station. The models were built and evaluated using data from calibration loading in both directions.

The regression equations are of the following form:

$$F_{HORZ/VERT} = a_1 * \epsilon_1 + a_2 * \epsilon_2 + a_3 * \epsilon_3 + a_4 * \epsilon_4 + b \qquad \text{(Equation 1)}$$

where ϵ_i represent the four strain gauge readings, a_i represent the four regression coefficients, and b is the regression intercept. For this equation, i ranges from 1 to 4 and corresponds to the strain gauge numbers shown in Figure 6.

The coefficient of determination R^2 was used to evaluate the accuracy of the models, where the quality of the fit improves as R^2 approaches 1.0. The worst performing cases using the single equation approach for F_{HORZ} and F_{VERT} regressions are shown below in Figure 11. The figures show the predicted loads from the linear regression models vs. target loads for all the calibration loads applied, and the corresponding R^2.

The horizontal load regression for the upper lug at FS470 and the vertical load regression for the lower lug at FS453 were identified as the two regression models with the lowest coefficient of determination for each respective direction. These will be used as examples in the following sections to track changes in how accurate the models are.

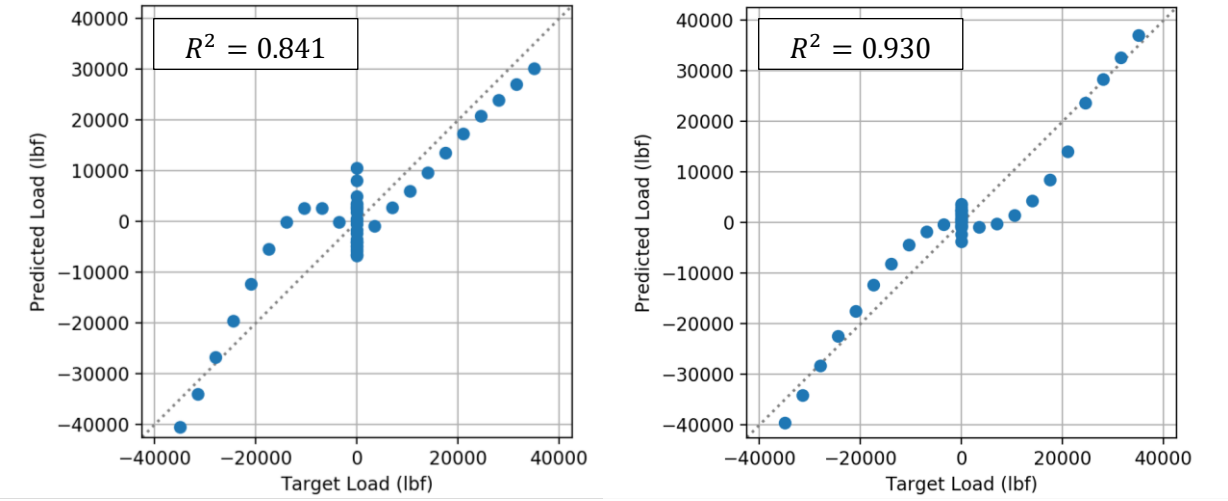

a) Horizontal load regression results for the upper lug at FS470

b) Vertical load regression results for the lower lug at FS453

Figure 11: Target vs. Predicted Loads of the Worst Performing Regressions

Positive/Negative Four-gauge Regressions

As previously noted, the strain gauges had very different responses to positive and negative loads in both directions. To account for this, two regression models were created for each location: one with positive calibration loads in the direction of regression and the other with negative loads. Both equations were derived using all of the calibration data in the other direction.

By splitting the model of F_{HORZ} for the upper lug at FS470 into two equations using only positive or negative calibration data in the direction of regression the results are improved. The regressions produce better predictions for the various calibration loads and are more linear than the first model.

It can be seen in Figure 12 that the vertical regression performed poorly for positive loads, and for this case, it seems that isolating it from the negative loads did not change or improve the performance of the models. The coefficient of determination increased from the single-equation for the negative F_{VERT} regression for the lower lug at FS453, but it decreased for the positive regression.

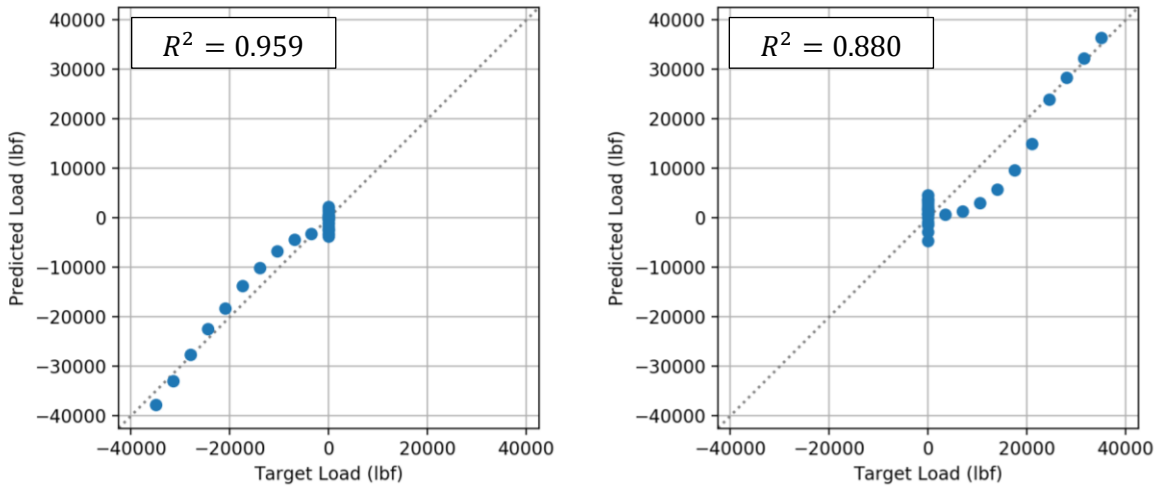

a) F_{VERT} regression using negative vertical load data

b) F_{VERT} regression using positive vertical load data

Figure 12: Vertical Load Regression Results for the Lower Lug at FS453

Four-Quadrant Four-Gauge Regressions

The lugs were likely to experience some combination of horizontal and vertical loads in testing. Based on the differing response to positive and negative loads seen in both directions, it was suspected that considering the sign of both load components may further improve the regression performance.

The four-quadrant approach was completed by splitting the positive and negative loads in both loading directions. Four equations were therefore produced at every location, each with a different combination of positive and negative calibration loads in the direction of interest as well as the other load direction.

From Figure 13, the approach shows improvements on both the single-equation and two-equation F_{HORZ} regressions for the upper lug at FS470, with higher coefficient of determination values than the previous methods.

Reviewing the values in Figure 14, the improvements of the four-quadrant approach in the vertical regressions for the lower lug at FS453 are not as consistent. In all of the plots, the diverging behaviour at the higher loads is concerning since these regressions may have to be extrapolated and they all begin to diverge which will affect the accuracy of load estimation. Although there are exceptions to this trend, it appears that separating the calibration loads into four-quadrants which each produce their own regression equations improves the performance and reliability of the models.

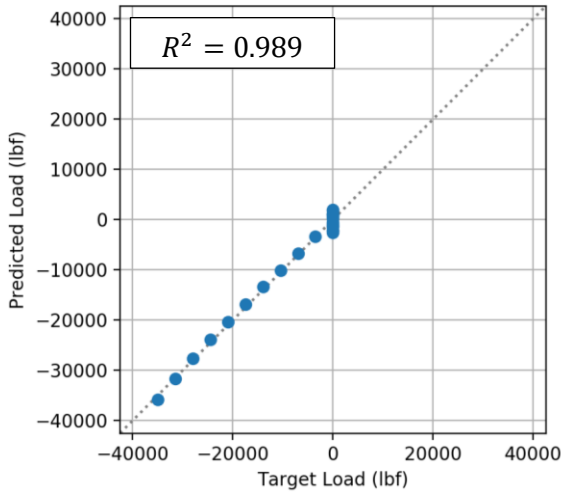

a) F_{HORZ} regression using negative horizontal load data and negative vertical load data

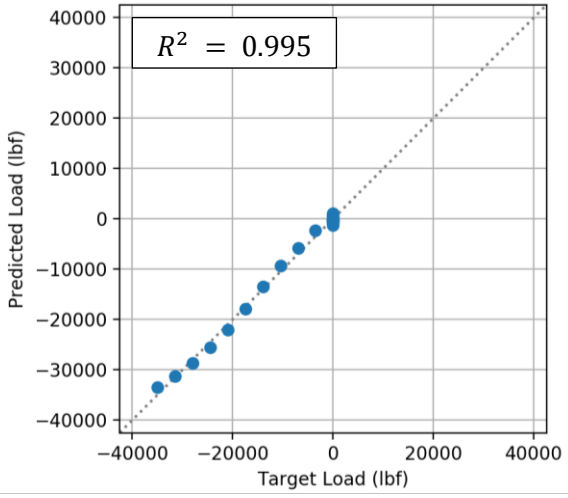

b) F_{HORZ} regression using negative horizontal load data and positive vertical load data

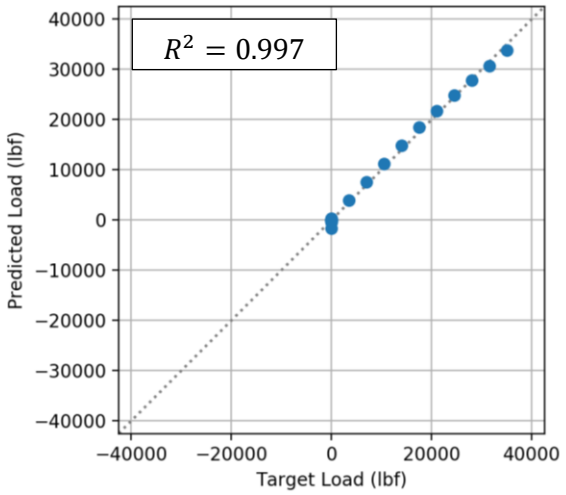

c) F_{HORZ} regression using positive horizontal load data and negative vertical load data

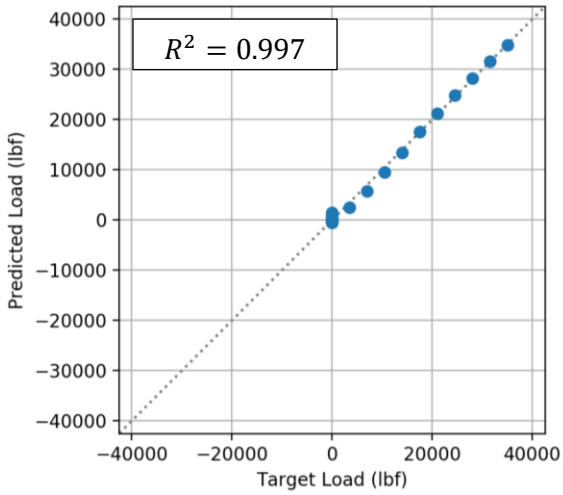

d) F_{HORZ} regression using positive horizontal load data and positive vertical load data

Figure 13: Four-Quadrant Horizontal Load Regression Results for the Upper Lug at FS470

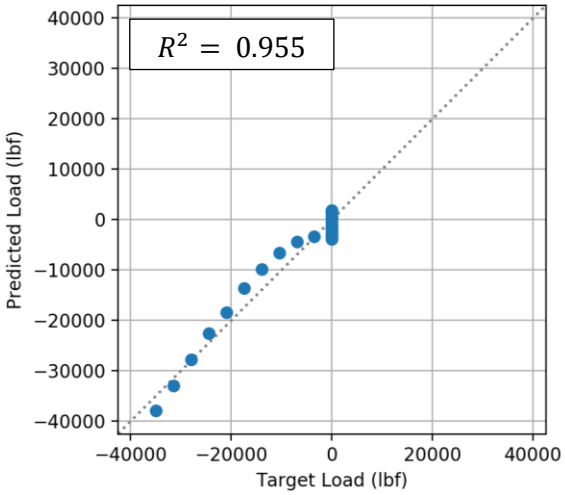

a) FVERT regression using negative horizontal load data and negative vertical load data

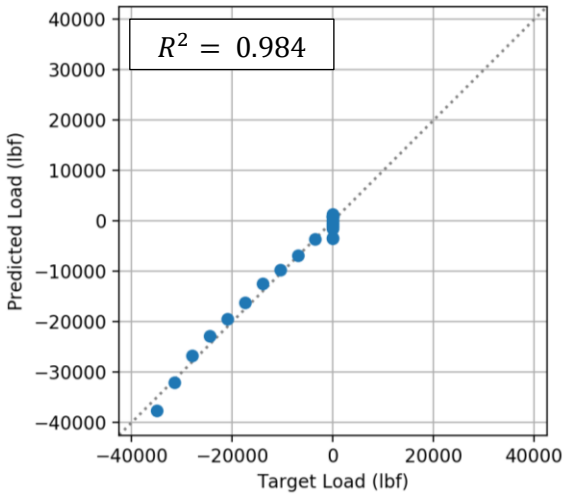

b) FVERT regression using positive horizontal load data and negative vertical load data

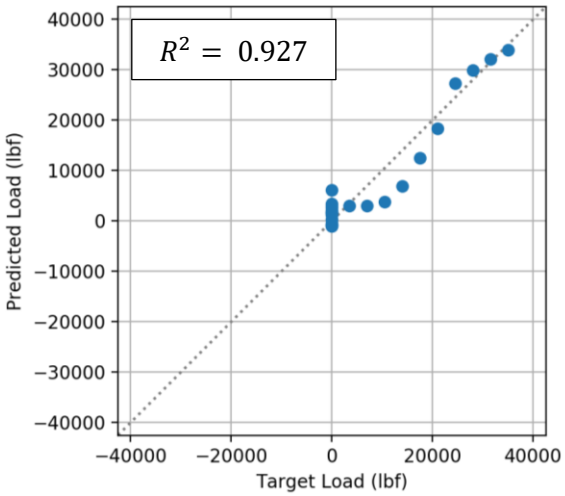

c) FVERT regression using negative horizontal load data and positive vertical load data

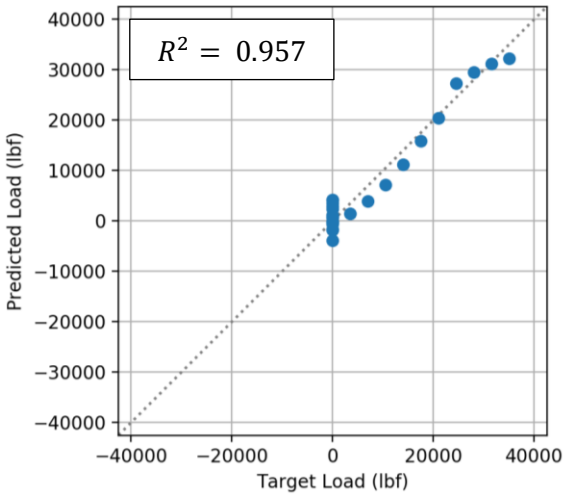

d) FVERT regression using positive horizontal load data and positive vertical load data

Figure 14: Four-Quadrant Vertical Load Regression Results for the Lower Lug at FS453

THREE-GAUGE REGRESSIONS

The motivation for the last approach came from two instances of interesting behaviour noted for Strain Gauge 2. In Figure 7, it can be seen that the strain readings extracted from the gauge locations for gauges 1, 3, and 4 display a sinusoidal behaviour in the various loading directions. However, at the location of Strain Gauge 2 the response was only approximately sinusoidal between 120 and 240 degrees; while everywhere else the strain readings were small. Also, the response of Strain Gauge 2 was most significant for negative horizontal loads while much lower in all other cases. For these reasons, regressions using only strains gauges 1, 3, and 4 were created to see if the input of Strain Gauge 2 was unnecessary or creating noise in the four-gauge regressions. The three previously mentioned approaches; single-equation, positive/negative, and four-quadrant regressions, were repeated using only the three gauges.

The regression equations are of the following form:

$$F_{HORZ/VERT} = a_1 * \epsilon_1 + a_3 * \epsilon_3 + a_4 * \epsilon_4 + b \qquad \text{(Equation 2)}$$

where ϵ_i represent the three strain gauge readings, a_i represent the three regression coefficients, and b is the regression intercept. For this equation, i can be 1, 3, or 4.

In general, the coefficients of determination were slightly lower for the three gauge regressions in comparison to the four-gauge regressions. Particularly the single-equation regressions performed poorly for most lug locations, for instance the single equation F_{HORZ} R^2-value for the upper lug at FS470 is 0.841 using four gauges and 0.449 using three gauges.

One of the issues that the three-gauge regression was attempting to address was the behaviour of the regressions at higher loads, since some of the four-gauge regressions diverge. Focusing on the four-quadrant approach, the horizontal load regressions from the three-gauge equations typically had behaviour on par or slightly worse at higher load magnitudes. For example, in Figure 15 it can be seen that the three-gauge regression has poorer predictions for higher target loads. For the vertical four-quadrant regressions, the behaviour was on par or slightly better. In Figure 16, the three-gauge regression seems to follow the dotted line more closely at higher target loads. This suggests that the three-gauge regression model is better at predicting higher loads than the four-gauge regression model. The three other vertical four-quadrant regressions using four- and three-gauges performed equally well at higher load magnitudes.

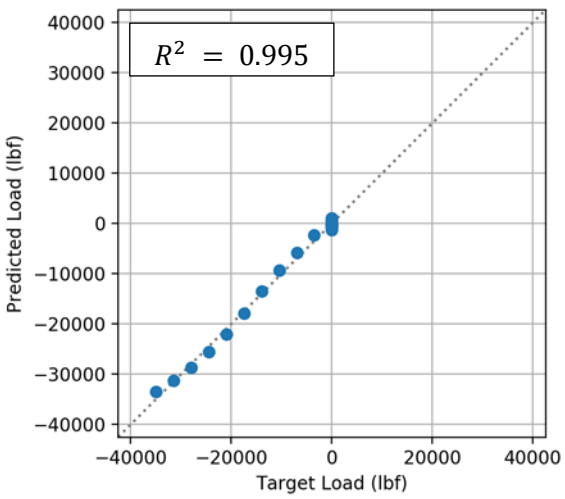

a) Four-gauge F_{HORZ} regression

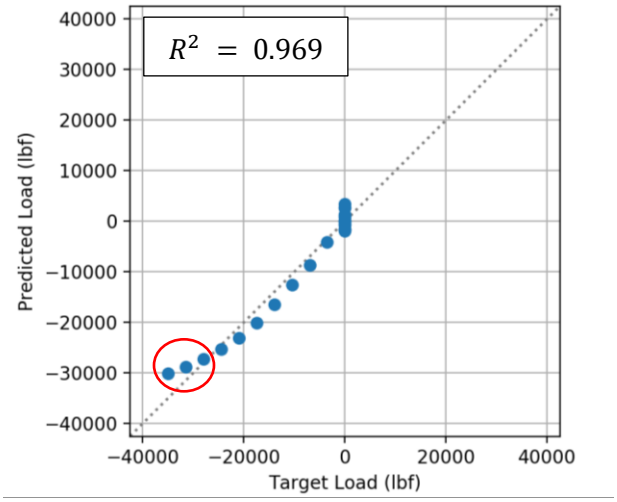

b) Three-gauge F_{HORZ} regression

Figure 15: Horizontal Load Regression Results Using Negative Horizontal Load Data and Positive Vertical Load Data for the Upper Lug at FS470

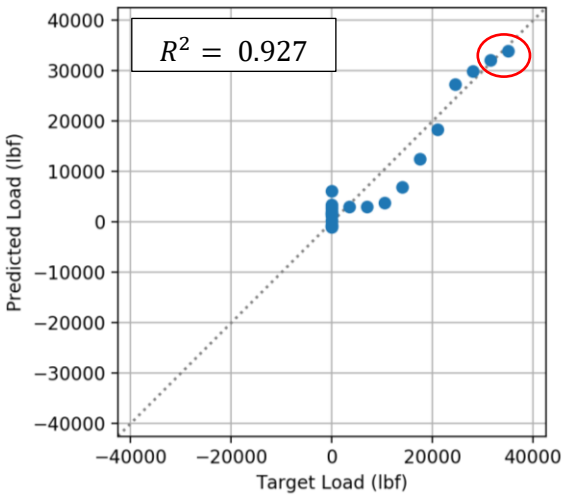

a) Four-gauge F_{VERT} regression

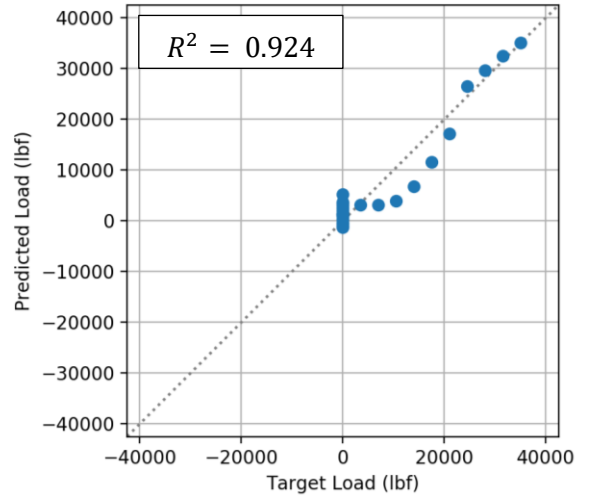

b) Three-gauge F_{VERT} regression

Figure 16: Vertical Load Regression Results Using Negative Horizontal Load Data and Positive Vertical Load Data for the Lower Lug at FS453

5. Application on ILEF Test Data

Calculation of Reaction Loads

Although the four-quadrant and positive/negative regressions generally showed better performance than single-equation regressions, a major issue arose: to be able to use the correct equation, the sign of the two estimated loads needs to be known, and since the loads themselves were not known neither were their signs.

To utilize all created regressions, an automated method for calculating the horizontal and vertical loads at each root lug was developed. This method uses the four-quadrant regressions whenever possible and the single-equation regression otherwise. The four-quadrant equations would not be used if the outputted loads contradicted the original signs of the calibration loads used to build the model. This method utilized the fact that Strain Gauge 2 showed small positive strains in response to positive horizontal calibration loads but significant negative strains to negative horizontal calibration loads.

The vertical and horizontal loads for the two lugs at each fuselage station were calculated using the following steps:

1. Using Strain Gauge 2 results, determine whether the horizontal load is negative or positive. If the strain is negative, the horizontal load is negative. If the strain is positive, the load is positive.
2. From the four-quadrant regressions, reduce the options being considered to those that agree with the sign of the horizontal load from the previous step. Using the two selected equations from the four-quadrant model, calculate the vertical load using each and eliminate the options that do not produce a load of the correct sign based on the data used to build the model.
3. Use one of the following options based on the results from the regression models:
    a. If the two regressions produce vertical loads of the correct sign, then select the option with a higher R^2 to find the vertical load.
    b. If only one is valid, use the valid equation to calculate the final vertical load.
    c. If neither have the correct signs, then use the single-equation regression to find the vertical load.
4. After the previous step, the vertical load should be determined. Based on the predicted sign of the horizontal load determined in the first step and the sign of the vertical load in the second step, use the four-quadrant F_{HORZ} equation trained on the correct sets of data to determine the horizontal load. If it produces a load with the incorrect sign, then use the single-equation approach to determine the horizontal load.

Wing Root Bending Moment and Torsion Comparisons

As a way to validate the accuracy of the load estimates, wing root bending moment and torsion were calculated using actual test data for the two specific load conditions inducing maximum and minimum WRBM respectively.

Bending moment and torsion were calculated using two approaches: a) using known actuator loads of each load condition and b) using the estimated reaction loads calculated using the root lug strain readings for these load conditions.

Table 1 summarizes ratios of estimated over actual wing root bending moment and torsion, derived from the estimated and the actual loads, respectively. The estimated bending moment was calculated using the horizontal reaction loads estimated with the 4-gauge regressions, as they had less divergence at higher horizontal loads than the 3-gauge ones. The estimated torsion was however calculated using the vertical loads estimated with the 3-gauge regressions, as they had less divergence at higher vertical loads than the 4-gauge ones.

Table 1: Ratios of Estimated over Actual Wing Root Bending Moment and Torsion

Load Condition	**Estimated ÷ Actual**	
	Bending Moment	**Torsion**
Min WRBM	0.560	-71.6
Max WRBM	0.729	-4.29

When comparing the bending moments created by the actuators to the values from the wing root lug gauge measurements, it can be seen that the bending moments experienced by the root lugs is smaller in magnitude than that produced by the actuators. This follows with the hypothesis that the drag load member was possibly experiencing loads in unexpected directions and carrying some of the bending moment created by the actuators. It is difficult however to prove that and it could only be one of the reasons for the discrepancies. There could be other structures that compensate for the difference, or it could be just an issue with underestimation of the loads for the root lugs due to some of the challenges experienced in the regressions and load selection.

Overall, the vertical loads were less consistent and reliable than the horizontal loads. It is difficult to say if any of the torsion values in the table above are accurate, as it is not clear if the vertical load values were correct. The estimated and actual torsion values are extremely dissimilar in magnitude and sign.

6. Concluding Remarks

To complete the ILEF fatigue test, a test rig structure was designed to meet the strength and fatigue performance requirements without failure. The resulting wing attachment lugs were manufactured in a much stiffer material than the actual fuselage bulkheads.

To determine the loads at the wing root interface, it was planned to install strain gauges on the root lugs (fuselage side), however it was also anticipated that the strain gauges may not be sensitive enough due to the high stiffness of the lugs. To improve the accuracy of the strain measurements, three-dimensional finite element analyses (FEA) of the stiffer lugs were performed to determine the optimum location of the strain gauges. The FEA process enabled the simulation of the calibration process, by applying calibration loads in the proper direction and evaluating the strain field at the surface of the part to instrument.

Using the strain gauge measurements and loads recorded during calibration, regressions for the horizontal and vertical load experienced at each lug were created. Models were built using multiple different sets of data and gauges. It was determined that the most reliable models were those built by splitting the calibration data in both direction by sign, and that the number of gauges used depended on the behaviour of the regressions at high loads. The four-gauge models

showed less deviation than the three-gauge at higher horizontal loads. However by removing Strain Gauge 2, the three-gauge models showed less deviation for the vertical load regressions.

Since it was not possible to calibrate the lugs using the full range of loads seen by the parts during test, the regression models were used to estimate values outside of the calibration range. This should be done with extreme caution, as the behaviour of these regression equations is unknown outside of this range. For example, with some of the models, increasing discrepancy between actual vs. estimated load was visible close to the highest calibration loads. It was not possible to quantify the discrepancy between actual and estimated load beyond the maximum calibration load. As a result, estimated loads for most – if not all – of the load cases applied during the test are questionable.

While creating the models, it was noted that the regression models provided typically less reliable results in the vertical direction than in the horizontal one. This was also true with the four-quadrant models, although the R^2 values were quite high for the regressions in both directions. As well, the vertical regressions were more likely to predict a load that contradicted the sign of the values used to build the regression. This led to a low level of confidence in the predictions. The possible reliability issues were supported by the torsion predictions, where the actual vs. estimated values were found extremely dissimilar in magnitude and sign.

The horizontal loads showed more reliable results in comparison. In contrast to the torsion values, the bending moments calculated from the actuator loads and from the estimated root lug horizontal loads were in better agreement in terms of magnitudes and signs. This result tend to support the hypothesis that the drag load member was actually reacting part of the horizontal loads. However, due to the issues seen in the load selection process and the unknown reliability of the extrapolation, it is hard to conclude if the differences in bending moments were only caused by the load transferred through the drag load member.

Although not entirely successful in this case, the methodology developed during this project is highly valuable, as it enables proper selection of gauge locations. Based on the results from this exercise, it is recommended to calibrate the instrumented component using the full range of loads, whenever possible, to avoid extrapolating results.

7. Acknowledgement

This work was carried out under contract with the Royal Canadian Air Force.